NUMERICAL INVESTIGATION OF PROGRESSIVE DAMAGE AND THE EFFECT OF LAYUP IN NOTCHED TENSILE TESTS

STEPHEN R. HALLETT* AND MICHAEL R.WISNOM

Department of Aerospace Engineering, University of Bristol,

University Walk, BS8 1TR, UK

SUMMARY: This paper presents results from a new approach to finite element modelling of notched damage in composite materials using interface elements to model intra- and inter-ply damage. The technique is used to examine and predict the failures observed in tensile, double edge notched specimens using four different layups made up from glass/epoxy prepreg. Due to the detailed modelling of the individual damage modes their interaction is well characterised. The analytical results obtained compare well with detailed test observations, capturing delamination and intra-ply splitting. By including the sub-critical damage that occurs at the notch tip in the model, the stress singularity is removed and failure criteria can be used to predict ultimate ply failures.

KEYWORDS: Notched strength, progressive damage, finite element analysis, interface element

* Author to whom correspondence should be addressed.
E-mail: stephen.hallett@bristol.ac.uk tel:- +44 117 3317098 fax:- + 44 117 927 2771

INTRODUCTION

The subject of damage in notched composites is an area of extensive research. A highly detailed analysis is required to accurately predict stresses in the region of a notch tip[1,2]. For sharp notches finite element analysis shows a stress singularity at the notch tip. This results in arbitrary values, which are dependent on mesh size, being predicted for the maximum stress in the load bearing plies. In reality the stress levels at which ultimate failure occurs are modified by the presence of progressive damage, which develops in the specimen from relatively low levels of applied load. This takes the form of splitting within the plies in the loading direction at the notch tip, matrix cracking transverse to the load and delamination between the plies. An experimental investigation by Kortschot and Beaumont[3] has provided a description of this damage and the failure patterns for cross-ply laminates. This has been extended to other layups by Hallett and Wisnom[4] and other authors[5,6,7].

One approach to determine notched strength has been to use the point or average stress at a characteristic distance from the notch tip as proposed by Whitney and Nuismer[8]. Many variations of such failure criteria have been put forward but a general short coming of such approaches is that they require experimentally determined parameters that are layup specific. Kortschot and Beaumont[9] have used finite element models with damage inserted at appropriate locations to obtain the relation between stress and damage and subsequently used this in expressions to predict how the damage will initiate and grow. An alternative approach is to include the damage prediction in the finite element model such as has been done by Chang and Chang[10], using a set of interactive failure criteria followed by property degradation to predict progressive damage growth and residual strength in open hole tension tests. Coats and Harris[6] have used a stress based progressive damage model to predict matrix cracking and

fibre failure. Delamination was not included and results were significantly mesh size dependant, however once this was calibrated against a single test result good predictions were obtained for residual strength of a centrally notched specimen over a range of specimen sizes and notch to width ratios. Methods such as these include the damage modelling in the continuum elements used to model the plies but do not explicitly take account of the splitting and delamination that occurs as sub-critical damage. Kwon and Craugh[11] have included a thin "delamination layer" at the 0/90° interface of a notched cross-ply model that shows reasonable predictions for the shape of delamination. Iarve et al[12] have compared analytical predictions and experimental observations of the strain field at an open hole with an associated intra-ply split. This has shown that modelling of the split by property degradation of elements does not give good results. The physical discontinuity due to the ply split needs to be included in the model in order accurately predict the strain distribution.

The interface element approach is one method of inserting a discontinuity into a finite element model. This approach has been developed largely to model delamination in composites[13,14,15]. This technique has the advantage that it can be used to predict both the initiation and progression of the delamination. It does however require an a-priori knowledge of the potential failure sites and elements to be inserted along such a path. Good results can be achieved for single and mixed mode loading and analyses have been correlated for example with end notch flexure (ENF), double cantilever beam (DCB) or mixed mode bending (MMB) tests[16].

Previous work has used the interface element technique to predict both the delamination and splitting prior to ultimate failure[17] in cross-ply laminates. Here this has been extended and applied to four different layups. The effect of inclusion of sub-critical damage in the model on

prediction of ultimate strength and failure mode by a simple strain based criterion has been examined.

EXPERIMENTAL RESULTS

Quasi-static tensile tests have been conducted using Hexcel E-glass/913 double edge-notched specimens. The results from these tests have been extensively reported in reference 4 and are only briefly summarised here. Scaled tests giving widths of 10, 20 and 40mm were performed for each lay-up. Of the available data, the 20mm wide specimens were chosen for comparison with the analytical results. The specimen geometry and layups tested are shown in Figure 1.

The damage development was monitored from the start of loading and its growth was recorded using a digital video camera. Figure 2 shows some typical results from the 20mm wide specimens of all four lay-ups tested. The images shown are not taken at regular time intervals but have rather been chosen to best show the damage development.

Damage initiates at the notch tips in the form of clearly visible splits within each ply, extending in the fibre direction. This occurs at a relatively low stress compared to the ultimate failure load. Additional intra-ply matrix cracks develop transverse to the applied load in the central section. Adjacent to the splits are areas of delamination, seen as darker areas in Figure 2. The ultimate tensile strength of the specimen is controlled by fibre failure except in the case of the $[45/90/-45]_s$ laminate where smaller specimens failed by delamination and fibre pull-out only.

FINITE ELEMENT ANALYSIS

Finite element analyses of the 20mm wide tests have been conducted using the explicit code LS-Dyna. The models were built up from stacked shell elements, with each ply within the laminate being modelled with a separate layer. Since each laminate is symmetric, only a half model through the thickness was used. To model delamination between the plies in the region of the notch, interface elements have been used, the formulation of which is described later in this paper. In order to connect the plies with interface elements it is required that adjacent plies have coincident nodes. It is therefore a quasi - two dimensional analysis which ignores through thickness tension and compression due to lack of offsets between the plies. This was felt to be an acceptable simplification since the delamination is primarily driven by shear. A linear elastic analysis has further been used to examine differences in fibre direction stresses between quasi-two dimensional shell and three dimensional brick models. Significant differences were not observed for thin laminates such as those examined here. Figure 3 shows a schematic view of a typical model ($[+45/90/-45/0]_s$ layup) and boundary conditions together with interface element locations. In addition to the delamination damage between plies, splitting within each ply has been modelled using interface elements. Again coincident nodes are required and these have been inserted in each ply in a line extending from the notch tip in the fibre direction. Experimental work has shown this to be the predominant site of split locations. Without the inclusion of this sub-critical damage, the stress state at the notch tip would form a singularity and hence the values obtained would be mesh dependent, making it difficult to incorporate failure criteria. The interface element approach overcomes this limitation and allows the detailed damage development to be included in the model using only elastic material properties, non-linear shear behaviour, G_{Ic}, G_{IIc} and the matrix failure stress, all of which can be obtained experimentally.

Figure 4 shows experimental and numerical results of a 20mm wide cross-ply specimen all at 200MPa applied far field stress. Figure 4b shows the splitting and delamination damage predicted by failure of interface elements and Figure 4c shows the 0° fibre direction stress distribution. By comparison the fibre direction stress distribution in a model that has no interface element failure (Figure 4d) shows a highly localised stress concentration with a maximum value in excess of the unidirectional fibre failure stress[18]. The sub-critical damage clearly has an effect of blunting the notch, cause a redistribution of stress. This is significant for predicting failure of the load bearing plies since if stress or strain based criteria (as are commonly implemented in finite element codes) are used, the model without any sub-critical damage will be predicted to fail at applied stress levels well below those observed in tests.

The angle of the notch (θ) in the tests was 60°. Analysis showed no difference in results between a sharp notch (θ = 0° as modelled in reference 17) and an angled notch as tested, since the sub-critical damage modifies the stress field as soon as the split initiates. The angle of the notch in the modelling work presented here is for visualisation only and therefore 45° has been used in order to make it easier to preserve a regular mesh of 0.25 × 0.25mm in the area of interest. Since LS-Dyna is an explicit code it is better suited to modelling of dynamic events of very short duration. Quasi-static events can however be modelled if sufficient care is taken to ensure that dynamic effects are not significant. In order to ensure that the analysis completes in a reasonable time, a number of techniques are employed to reduce the CPU time taken. The analysis is run at a faster loading rate than the test, mass scaling is used to increase the timestep and damping is employed. The kinetic energy of the system is carefully monitored throughout to ensure that these changes have minimal effect. Additionally analyses

have been conducted at varying loading rates and levels of mass scaling to ensure results are not affected by these procedures.

INTERFACE ELEMENTS AND SUB-CRITICAL DAMAGE

The interface element is essentially a 3 degree of freedom non-linear spring with interaction between the degrees of freedom. The initial spring stiffness is calculated from an assumed resin rich layer 0.005mm thick, a nodal area calculated from the area of the shell elements attached to each node and a Young's modulus of 4GPa which is typical for epoxy resin. For ease of calculation a uniform element size has been used in the area of delamination and splitting. For the elements representing the delamination damage, only shear failure needs be considered since through thickness effects and hence mode I type failure are ignored. The shear properties of the element are assumed to be uniform in every direction on the shear plane and equivalent to a mode II type failure. The response of the interface element to an applied displacement can be seen in Figure 5a. The equivalent force - relative displacement response remains linear until a maximum is reached after which the slope is reduced such that the area under the curve is equal to the mode II fracture energy for the element concerned. The element is assumed to have failed when the force reaches zero. Previous work[17] used a perfectly plastic post yield behaviour instead of work softening. A study was done for both the work softening and perfectly plastic behaviour. Both analyses give similar results with the work softening behaviour leading to greater numerical stability since there is not a sudden reduction in force at each interface element failure. The maximum force for each element in the current analysis was calculated from a strength value of 75MPa[17].

For a cross-ply lay-up loaded orthogonally to the fibre directions it is sufficient to use the same one dimensional interface element for the intra-ply splitting as for the delamination since there is only mode II loading[17]. In order to extend the analysis to lay-ups other than cross-ply, mixed mode behaviour was included in the interface element. Mode I and mode II energy components are combined using equation 1 and failure occurs when the left hand side is equal to 1.

$$\left(\frac{G_I}{G_{I_c}}\right)+\left(\frac{G_{II}}{G_{II_c}}\right)\leq 1 \qquad \textbf{Equation (1)}$$

The maximum force for the mixed mode case is based on the Von Mises yield criterion. The subject of mixed mode loading has been given much consideration in the literature with the majority of work being done on delamination. In the current model mixed mode loading occurs only in the splitting but this is thought to be very similar to delamination growth as both occur in the resin regions between fibres. After the Von Mises criterion is exceeded, the resultant force in the interface element is reduced such that equation 1 is satisfied. Figure 5b gives a graphical representation of the equivalent force - relative displacement behaviour of the interface element under mixed mode loading conditions.

The mode ratio will not necessarily remain constant throughout the period of loading of a single interface element. If this changes, the area under the equivalent force - relative displacement curve (and hence the energy) is accounted for by adjusting the softening gradient. This allows for small changes in loading direction, ensuring the energy balance is maintained. It is not a completely general solution since once softening has initiated the force in the interface element cannot increase. It was felt to be adequate since large changes in mode ratio were not observed in individual interface elements. The mode ratio is of course

permitted to change as the split extends during damage development and different interface elements fail.

Predicted damage has been compared to the test results in terms of split length and delamination location. Figure 6 shows that relatively good correlation has been achieved for growth of the 0° ply split in the cross-ply specimens. Correlation was found to be worst at the split initiation point. This may be due to residual stress from the curing process or machining defects from the cutting of the notch, which are not taken into account in the model. As the growth of the split progresses, the correlation improves. It can be seen that the analytical split growth rate is strongly dependent on the value of G_{IIc} used. Due to previously discussed similarities in the damage process between splitting and delamination and difficulties in obtaining experimental data for the fracture energies is has been assumed sufficient to use the same data for both the splitting and delamination interface elements. Here two values taken from the literature have been used, 1.08N/mm (reference 19) and 0.9N/mm (using an average of the results presented for differing adjacent ply angles in reference 20), with the lower value giving better correlation for final split length. It is possible that using a single value for the fracture energy as the split grows is not sufficient and will cause a variation in correlation due to the R-curve effect. Wisnom and Chang[17] found that it was necessary to include the non-linear shear behaviour of the material in the model in order to achieve good correlation for the split growth. A piecewise linear curve fit to the data from reference 21 has been used here and is shown in Figure 7 together with a sub-set of the test data. G_{IC} is not a critical value for the delamination or splitting in the cross-ply specimen but is required for splitting in the other laminates modelled. A value of 0.25N/mm[19] was used. The ply elastic material properties are shown in Table 1.

Figure 8 shows the sub-critical damage results near to the mean experimental failure load from analyses for the different lay-ups that were tested. Photographs of a typical 20mm wide specimen are shown at the same scale from a representative test at the same applied stress. For the cross-ply lay-up a half model was used. For those lay-ups that contained ±45° fibres a full model was used since there is no true plane of symmetry due to the layup. It can be seen that there is generally good agreement in both the location and extent of delamination and splitting. Comparison with tests at exactly equivalent positions during loading is difficult due to the scatter in test data. In the experimental photographs it can be seen that in addition to the major splits starting from the notch tip there are a significant number of other matrix cracks in the laminates. Uniformly distributed matrix cracks have been reported as the site of delamination initiation[22]. Experimental evidence suggests that for the notched case the significant delamination grows from the intra-ply splits associated with the notch tip. The matrix cracks observed in the material in the region between the notch tips do not have a significant effect on this delamination growth.

In all of the lay-ups damage initiated at the notch tip by splitting which agrees well with the experimental observations presented in reference 4. In order for the split to propagate in the fibre direction of each ply at least one of the delamination elements attached to the same nodes must also fail to allow relative displacement of the two split element nodes. Split growth rates in each of the 45, 90, -45 and 0° directions was not necessarily equal. Once the splits had started to propagate away from the notch tip into the specimen, triangular regions of delamination began to form between adjacent splits. These are shown in Figure 8 at the individual interfaces which when overlaid on top of each other combine to give the equivalent picture to that observed experimentally.

ULITIMATE FAILURE MODELLING

The model described above was used to examine the final failure modes predicted when a ply failure criterion was introduced. Complete ply failure as a result of fibre failure was included by means of a quadratic criterion between fibre direction and shear response. This was implemented as a strain formulation (equation 2) in order to better take account of the non-linear shear behaviour. Once this criterion is exceeded in a given element it is deleted from the analysis.

$$\left(\frac{\varepsilon_1}{\varepsilon_{1C}}\right)^2 + \left(\frac{\gamma_{12}}{\gamma_{12C}}\right)^2 \leq 1 \qquad \textbf{Equation (2)}$$

The fibre direction tensile failure strain (ε_{1C}) was obtained from careful testing of UD specimens that were waisted in the thickness direction by dropping plies[23]. A mean value of 3.5% was obtained for specimens with four and eight plies in the gauge length[18]. A value of 5% was used for shear failure strain (γ_{12C}) based on discussion in reference 21.

It is arguable that the transverse matrix cracking as seen in Figure 2 will affect the formation of delamination and splitting but in the analyses conducted here it was not felt to be significant since initiation is controlled by the location of the notch tip. This was backed up by analyses in which the elastic transverse modulus was artificially reduced, no discernable difference in damage pattern could be observed. The stress distribution within each ply however was more strongly affected since its load bearing capacity is influenced by the development of the matrix cracks. The reduction factor was calculated from the observed matrix crack density of 30 cracks/cm in cross-ply tests[4] and an analysis developed by Kashtalyan and Soutis[24] which predicts a 15% reduction in laminate axial stiffness. This

requires approximately a 50% reduction in stiffness of the 90° plies from the value quoted in table 1. This reduced stiffness was not included in the previous analysis for sub-critical damage since it did not affect the extent of splitting and delamination but has been included in analyses for ply failure.

Looking only at the maximum applied far field stress at failure for the 20mm wide specimens it can be seen that there is relatively good agreement between test and analysis for the first three layups (Figure 9). The final layup shows worse correlation to test and this is attributed to the different failure mode that was observed in this layup compared to the others. Each layup analysed warrants further discussion with respect to the failure mode and its comparison to test.

Figure 10 shows the final failure for the test and analysis of the cross-ply layup. The finite element result shows only a close up of the 0° ply with the failed elements removed (using equation 2). The experimental result shows all plies with the damage highlighted using strong backlighting. Ultimate failure in both the test and analysis occurs across the width of the specimen starting at the notch tip with failure of the 0° fibres. This rapidly progresses across the width of the specimen. The fibre-failure observed in tests is not exclusively orthogonal to the loading direction as can be seen in Figure 10, but progresses at an angle away from the notch tip, indicating an influence of shear stress. This is accompanied by additional splitting and delamination similar to that seen before the fibre failure. The model does not have the capacity to capture these further splits and this may be the cause of the differences in the failure patterns observed. The model takes account of the direct and shear stress interaction through the relationship in equation 2 and it is this interaction that causes the path of failed elements to progress in the fibre direction rather than directly across the specimen width. The

direction of fibre failure is somewhat different to that observed in test where it is at approximately 45° to the notch tip. Further work is required to investigate the detailed nature of the stress interaction in order to improve correlation.

The test results for the $[+45/90/-45]_s$ layup showed two possible failure modes. The first showed considerable amounts of delamination but the catastrophic failure of the specimen was due to failure of the fibres across the specimen width. The second mode was failure by delamination only and the plies pulling out from between each other without fibre failure. This can occur since there are no 0° plies in this layup. The first mode is captured well by the analysis and comparison with a test that exhibited this mode is shown in Figure 11.

Tests on the $[+45/90/-45/0]_s$ layup show fibre failure to occur across the width of the specimen and also some fibre pull-out and some delamination back towards the specimen grips once the fibre failure has extended more than half way across the specimen width (Figure 12). The analysis predicts fibre failure in all plies in a band which closely approximates the area of failure observed. A slightly surprising result was the failure of the 90° ply by fibre failure in the finite element model as well as splitting in the fibre direction by failure of the interface elements (a site of potential splitting has been modelled starting from the notch tip). This has been confirmed to occur in the tests by thermal de-ply of the failed specimens which does indeed show some of the 90° plies to have failed in a very similar manner, initially splitting and then fibre failure at an angle to the fibre direction[4].

Tests on the $[+45/90/-45/0_2]_s$ layup showed a different failure pattern to that observed in the other layups. Only the internal -45° plies failed at the point of maximum load. On continuation of loading the central 0° plies separated from the adjacent plies by splitting and

delamination and continued to carry load until they failed by distributed fibre failure that was not affected by the position of the notch (Figure 13).

Figure 14 shows that the analysis predicts fibre failure in the –45° ply but also in all of the other plies. This is possibly due to the fact that there is no capacity in the analysis to capture the distributed fibre failure that was observed in the tests. Additionally the extensive delamination back to the specimen grips was not predicted by the analysis although the damage prediction at 70% of the mean test failure load was reasonable (Figure 8). Once the sub-critical damage has progressed a significant amount, the assumption of quasi-two dimensional behaviour may no longer be sufficient. Asymmetric sub-laminates will be formed by the existence of the delamination and significant out of plane forces may develop which will contribute to further extension of the delamination and ultimate separation of the specimen. The analysis will under predict the amount of delamination since is does not take account of mode I opening of the delamination. The ultimate failure stress prediction for this layup (Figure 9) is somewhat below the mean test value, a result of the under prediction of the "blunting" effect caused by splitting and delamination. Correct prediction of the delamination may prevent premature ply failure. Work is on-going to investigate the use of fully three dimensional models for the prediction of such delamination.

MESH SENSITIVITY

A significant problem with the modelling of material failure by finite element methods is that the resulting strength predictions can be dependent on the mesh size used. This makes the development of a general model that can be applied to different size specimens and different layups extremely difficult. A study was run on the $[90/0]_s$ layup in which the mesh size was

increased and decreased from the “base” analysis (0.25mm square mesh) to double and half its size. Examining only the ultimate failure stress it can be seen from Figure 15 that whilst there is some variation, all results are within 10% of the mean test result.

However if the predicted sub-critical damage is examined at the same applied stress level, as has been shown in Figure 16, it can be seen that the “base” and “fine” meshes are in good agreement but the “coarse” mesh has a considerably reduced damage area. There is an upper limit on the mesh size that can be used for the interface elements beyond which the damage will not propagate due to the high forces required for modelling the softening behaviour. The area of each interface element and hence the maximum force increases with the mesh size. At large sizes there is no longer sufficient stress concentration to initiate softening. This impedes the growth of the damage in the coarse mesh. The fact that the ultimate failure stress is reduced from that of the base mesh is due to the reduced amount of splitting and hence notch blunting that occurs. The good agreement between the “base” and “fine” meshes in Figure 16 indicates that once this threshold has been passed, mesh size dependencies are greatly reduced for the sub-critical damage prediction. Similar behaviour has been observed in other interface element studies[25] with coarser meshes requiring greater applied loads for propagation due to the reduced number of elements in the cohesive zone.

The reduction in ultimate failure stress from the base mesh to the fine mesh indicates that there is still a small mesh dependency in the ply failure prediction. This mesh dependency is however considerably less significant than if the sub-critical damage had not been included in the model.

DISCUSSION

An analysis technique has been successfully developed that predicts the detailed development of sub-critical damage in notched laminates for layups that include ±45° plies. The effect of this damage on the stress distribution and final failure due to the inclusion of a ply failure criterion has been examined. The approach closely represents the physical mechanisms observed in the tests, and is able to predict failure of different layups from a single set of material properties that can be obtained from independent tests. The one layup that was an exception to this, $[+45/90/-45/0_2]_s$, exceeds the quasi-two dimensional assumptions made and exhibited a failure mechanism which thus far has not been included in the model. Mesh size has been shown to not be a significant issue for failure of the interface elements below a critical mesh size. The inclusion of the sub-critical damage reduces the stress singularity at the notch tip and allows the use of a ply failure criterion but does not completely eliminate mesh size effects for the failure of the continuum elements. Examination of the final failure of the test specimens indicate that in some cases the analysis over predicts the amount of fibre failure. Whilst the assumption of mode II only delamination is sufficient when considering damage during its early stages of development it may not be adequate once the delamination has progressed sufficiently far such that the laminate is divided into two asymmetric sub-laminates. This will cause a mode I contribution to the delamination. An additional failure mode which has not been considered is the further splitting in the plies once fibre failure has started to occur. This will have a similar effect to the initial notch blunting and inhibit the progression of fibre failure in the plies. Both of these mechanisms will have an effect on the ultimate failure modes and the fibre failure that is predicted. Whilst the current model adequately predicts the early stages of sub-critical damage development these mechanisms

may have to be included to increase the ability to predict a greater range of failures in more complex laminates and loading scenarios.

CONCLUSION

It can be seen that the model presented gives an accurate description of the main failure modes prior to fibre failure, i.e. delamination and ply splitting, for a number of different layups and good correlation to test is achieved. In the case of the fourth layup this is limited to early stages of loading prior to the major delamination extending back to the grips. The damage has been modelled using only measured elastic material properties and fracture energies. A site of potential splitting and delamination does have to be assumed and interface elements inserted but their failure is predictive in nature. The importance of being able to model this damage is in the effect it has on the stress concentrations in the material. The splitting has an effect of blunting the notch which in turn affects the ultimate load carrying capacity of the material. This gives an improved accuracy to the finite element model for predicting ply failure since without this effect, failure would be significantly under predicted.

The main focus of this work has been the inclusion of the different damage modes that contribute to the ultimate failure. The final notched strength of an individual layup is dependent on the damage mechanisms that occur and their interaction, which have been modelled in detail. There is an equally complex interaction of stresses and the individual components have been predicted with greater accuracy due to the included damage.

This work has been funded by the U.K. Engineering and Physical Sciences Research Council under grant no. GR/N22519.

LIST OF FIGURES

TABLES

E_{11}	43.9 GPa
E_{22}	15.4 GPa
G_{12}	4.34 GPa
υ_{12}	0.3

Table 1 Elastic material properties for e-glass/913

REFERENCES

1 Kwon, S.W. and Sun, C.T. (2000) Characteristics of three-dimensional stress fields in plates with a through-the-thickness crack, *International Journal of Fracture,* **104**: 291-315

2 Hu, F.Z., Soutis, C. and Edge, E.C. (1997) Interlaminar stresses in composite laminates with a circular hole, *Composite Structures,* **37**: 223-232

3 Kortschot, M.T. and Beaumont, P.W.R. (1990) Damage mechanics of composite materials I: Measurements of damage strength, *Composites Science and Technology*, **39**: 289-301

4 Hallett, S.R. and Wisnom, M.R. (2005), Experimental investigation of progressive damage and the effect of layup in notched tensile tests, *Journal Of Composite Materials,* In press

5 Spearing, S.M., Beaumont, P.W.R. and Ashby, M.F. (1992) Fatigue damage mechanics of composite materials II: A damage growth model, *Composites Science and Technology*, **44**(2); 169-177

6 Coats, T.W. and Harris, C.E. (1999) A progressive damage methodology for residual strength predictions of notched composite panels, *Journal of Composite Materials*, **33**(23); 2193-2224

7 Harris, C.E. and Morris, D.H. (1985) Role of delamination and damage development on the strength of thick notched laminates, *Delamination and debonding of materials*, ASTM STP 876; 424-447

8 Whitney, J.M. and Nuismer, R.J. (1974) Stress fracture criteria for laminated composites containing stress concentrations, *Journal of Composite. Materials*, **8**: 253-265

9 Kortschot, M.T. and Beaumont, P.W.R. (1990) Damage mechanics of composite materials II: A damage-based notch strength model, *Composites Science and Technology*, **39**: 303-326

10 Chang, F.K. and Chang, K.Y. (1987) A progressive damage model for laminated composites containing stress concentrations, *Journal of Composite Materials*, **21**; 834-855

11 Kwon, K.Y. and Craugh, L.E. (2001) Progressive failure modelling on notched cross-ply fibrous composites, *Applied Composite Materials*, **8**; 63-74

12 Iarve, E.V., Mollenhauer, D. and Kim, R. (2003) Three-dimensional modeling and experimental investigation of damage accumulation in open hole composite laminates, *ICCM14*, San Diego

13 Allix, O. and Ladeveze, P. (1992) Interlaminar interface modelling for the prediction of delamination, *Composite Structures*, **22**: 235-242

14 Borg, R., Nilsson, L. and Simonsson, K. (2001) Simulation of delamination in fiber composites with discrete cohesive failure model, *Composites Science and Technology*, **61**: 667-677

15 Camanho, P.P., Davila, C.G. and De Moura, M.F. (2003) Numerical simulation of mixed-mode progressive delamination in composite materials, *Journal of Composite Materials*, **37**: 1415-1437

16 Borg, R., Nilsson, L. and Simonsson, K. (2004) Simulating DCB, ENF and MMB experiments using shell elements and a cohesive zone model, *Composites Science and Technology*, **64**; 269-278

17 Wisnom, M.R. and Chang, F.K. (2000) Modeling of splitting and delamination in notched cross-ply laminates, *Composites Science and Technology,* **60:** 2849-2856

18 Khan, B., Potter, K., Hallett, S.R. and Wisnom, M.R. (2004) Size effects in unidirectional composites and quasi-isotropic specimens in tension, *2nd International Conference on Composites Testing and Model Identification*, Bristol

19 Petrossian, Z. and Wisnom, M.R. (1998) Prediction of delamination initiation and growth from discontinuous plies using interface elements, *Composites: Part A*, **29**: 503-515

20 Shi, Y.B., Hull, D. and Price, J.N. (1993) Mode II fracture of+/- angled laminate interfaces, *Composites Science and Technology*, **47**: 173-184

21 Wisnom, M.R. (1994) The effect of fibre rotation in +-45 degree tension tests on measured shear properties, *Composites*, **26**(1): 25-32

22 Takeda, N. and Ogihara, S. (1994) Initiation and growth of delamination from the tips of transverse cracks in CFRP cross-ply laminates, *Composites Science and Technology*, **52**: 309-318

23 Khan, B., Potter, K. and Wisnom, M.R. (2005) Suppression of delamination at Ply Drops in Tapered Composites by Ply Chamfering, *Journal of Composite Materials,* In press

24 Kashtalyan, M. and Soutis, C. (2000) Stiffness degradation in cross-ply laminates damaged by transverse cracking and splitting, *Composites: Part A* **31**: 335-351

25 Turon, A., Dávila, C.G., Camanho, P.P. and Costa, J. (2005) An engineering solution for using coarse meshes in the simulation of delamination with cohesive zone models, *NASA Technical Memorandum 213547*

FIGURES

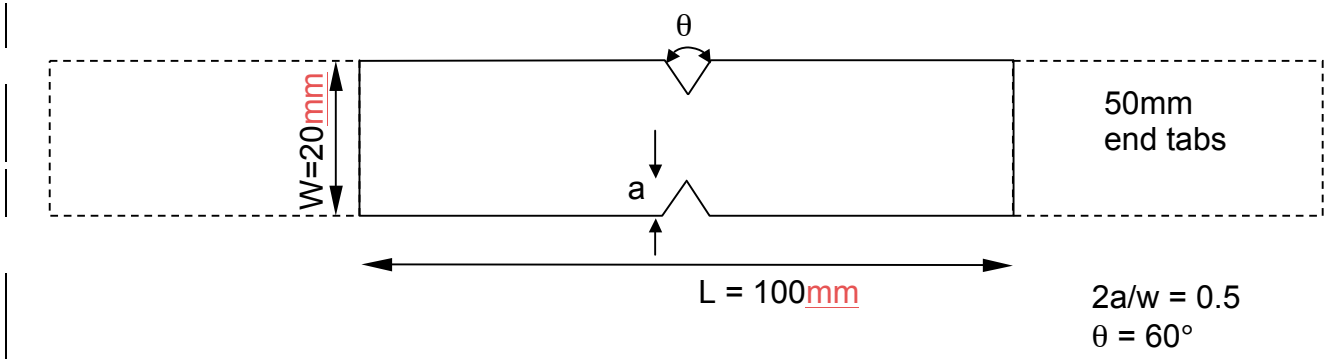

$[90/0]_s$
$[+45/90/-45]_s$
$[+45/90/-45/0]_s$
$[+45/90/-45/0_2]_s$

Figure 1 Specimen geometry

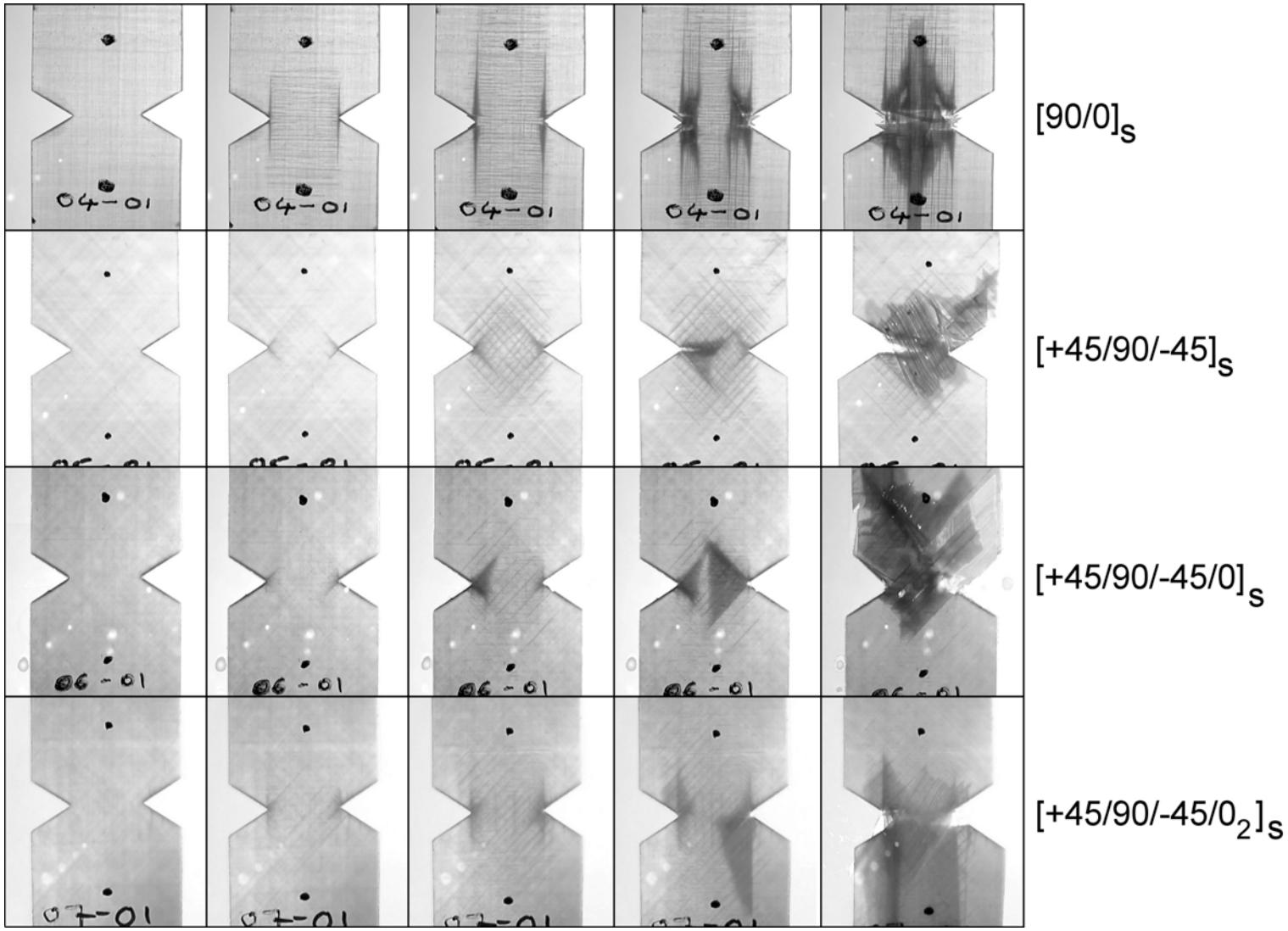

Figure 2 Typical results from the different layups tested

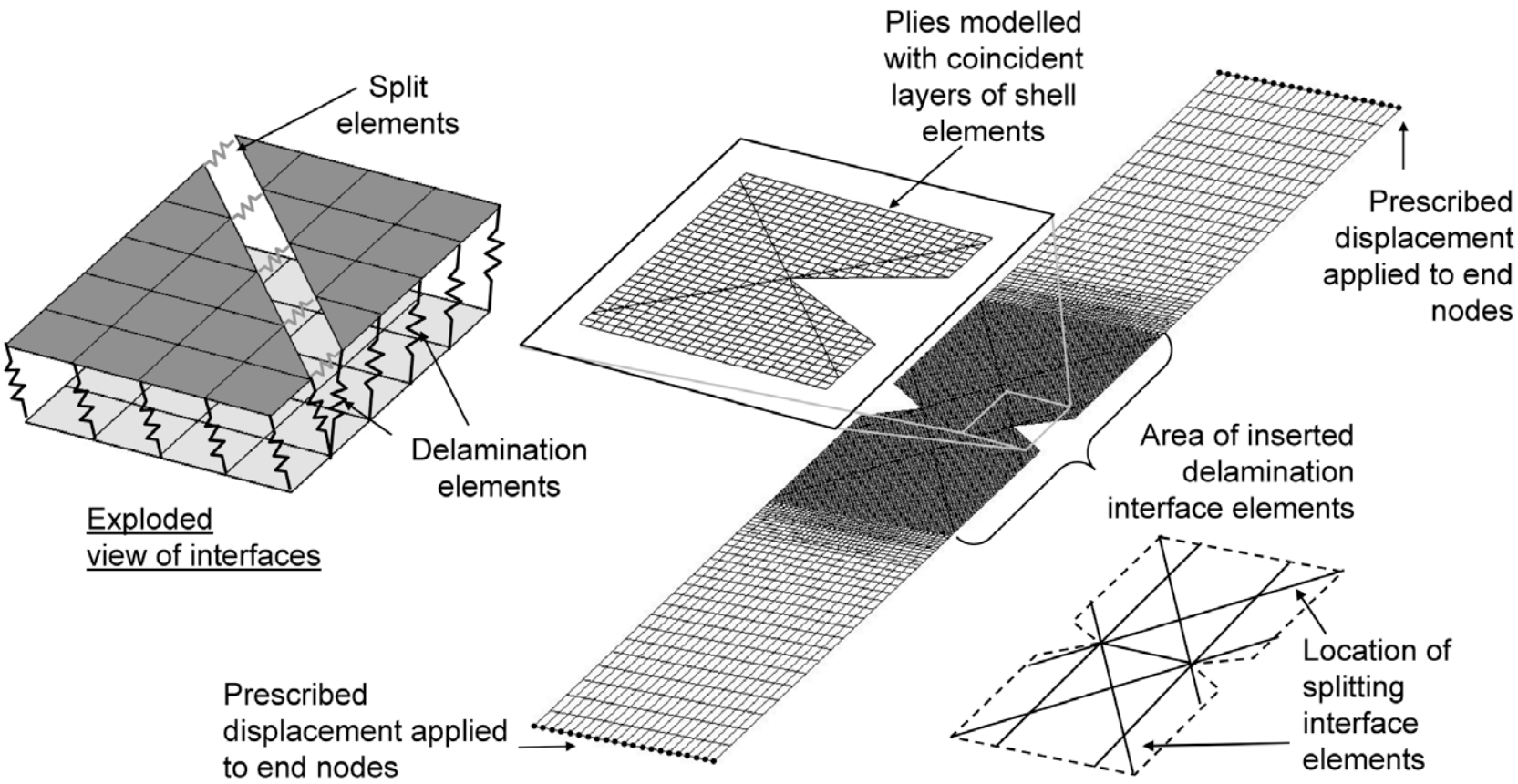

Figure 3 Schematic view of finite element model

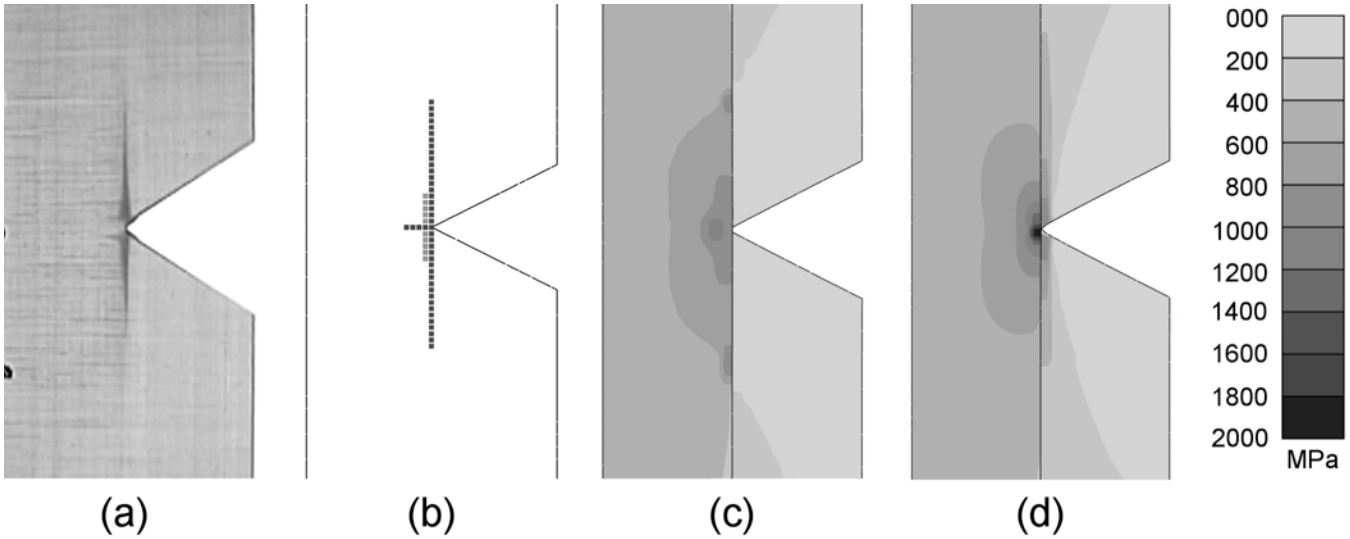

Figure 4 (a) Experimental damage, (b) predicted damage, (c) 0° stress distribution with damage, and (d) stresses without damage modelling, all at 200MPa applied far field stress[11]

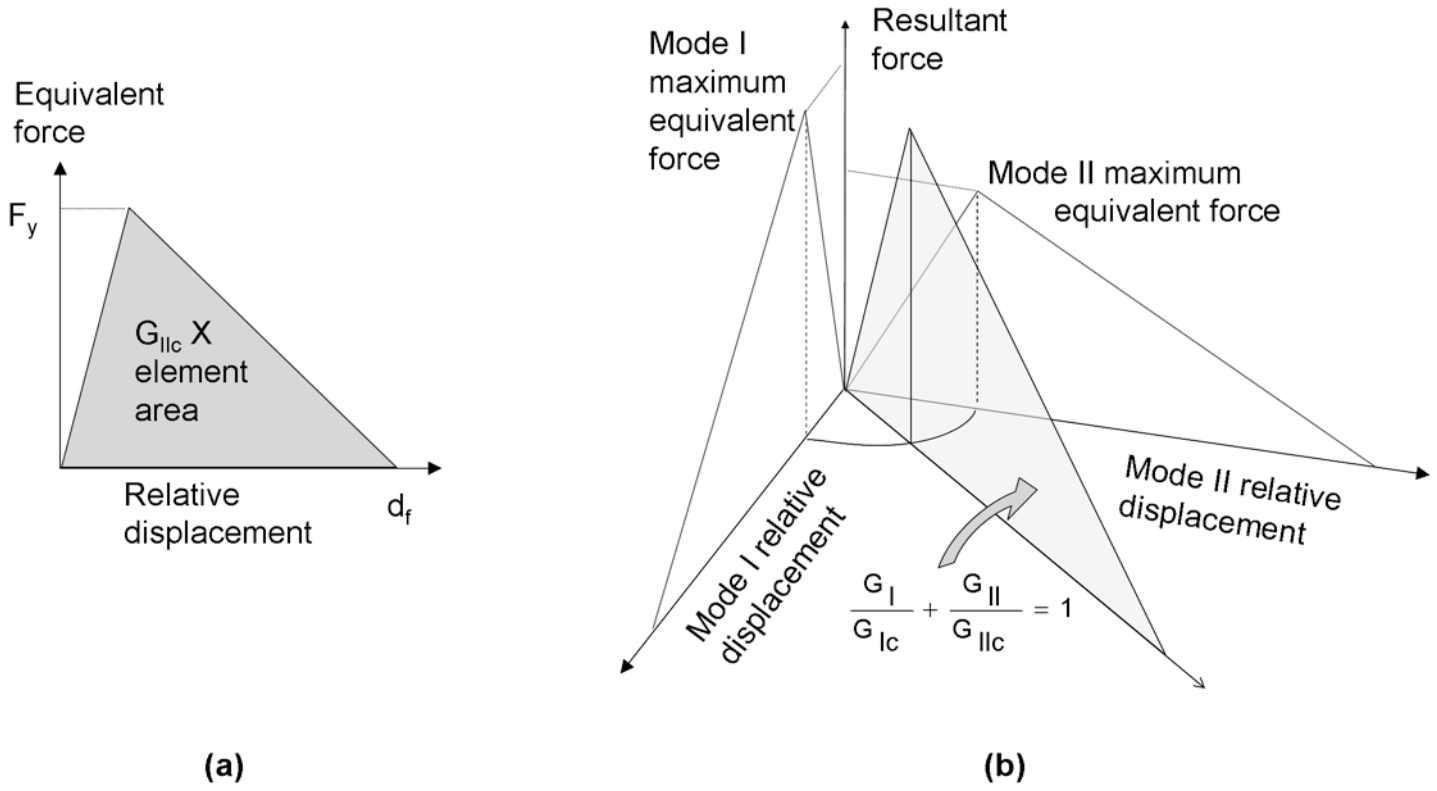

Figure 5 Equivalent force - relative displacement response for interface elements (a) mode II (b) mixed mode

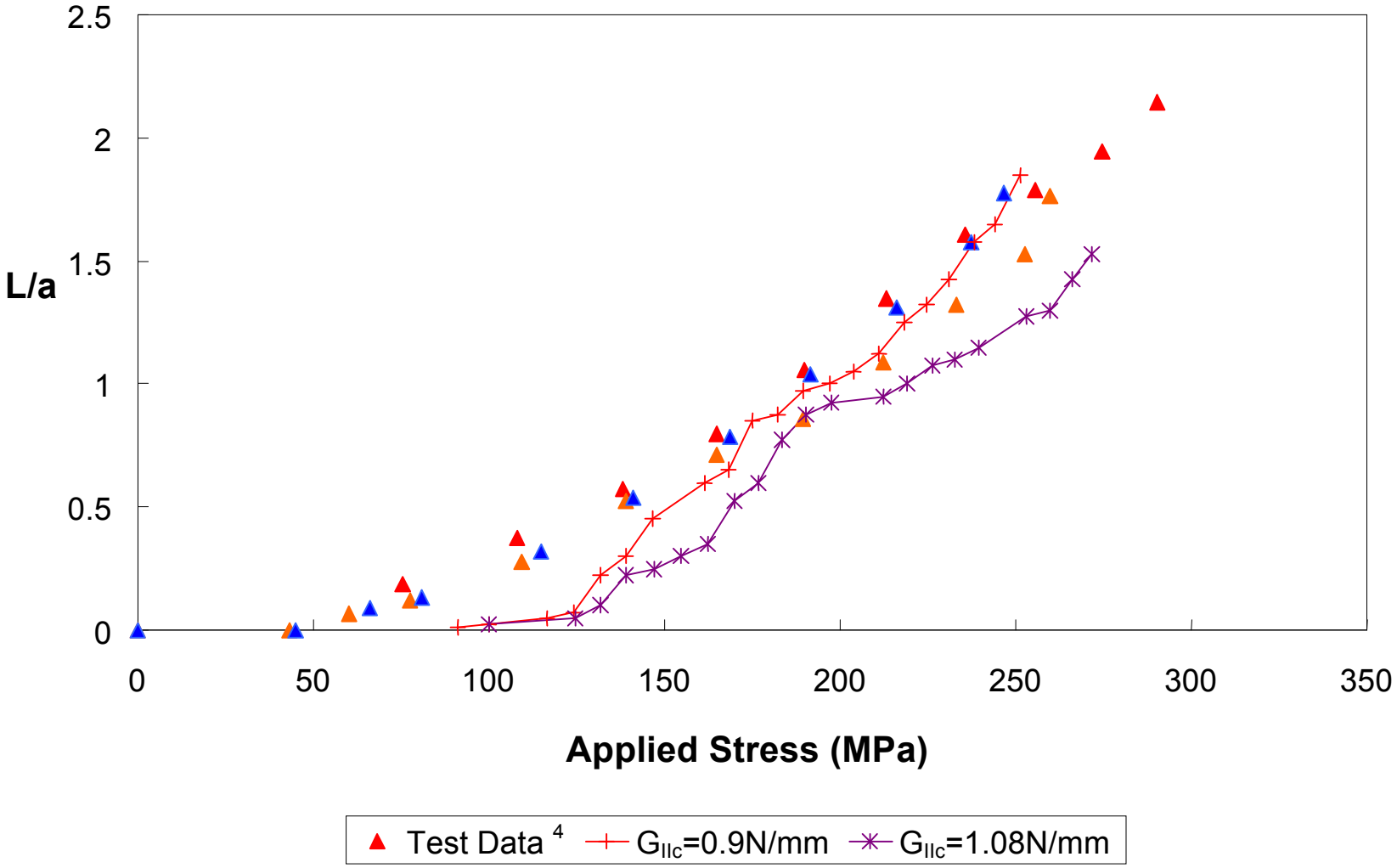

Figure 6 Split growth rate for cross-ply specimen

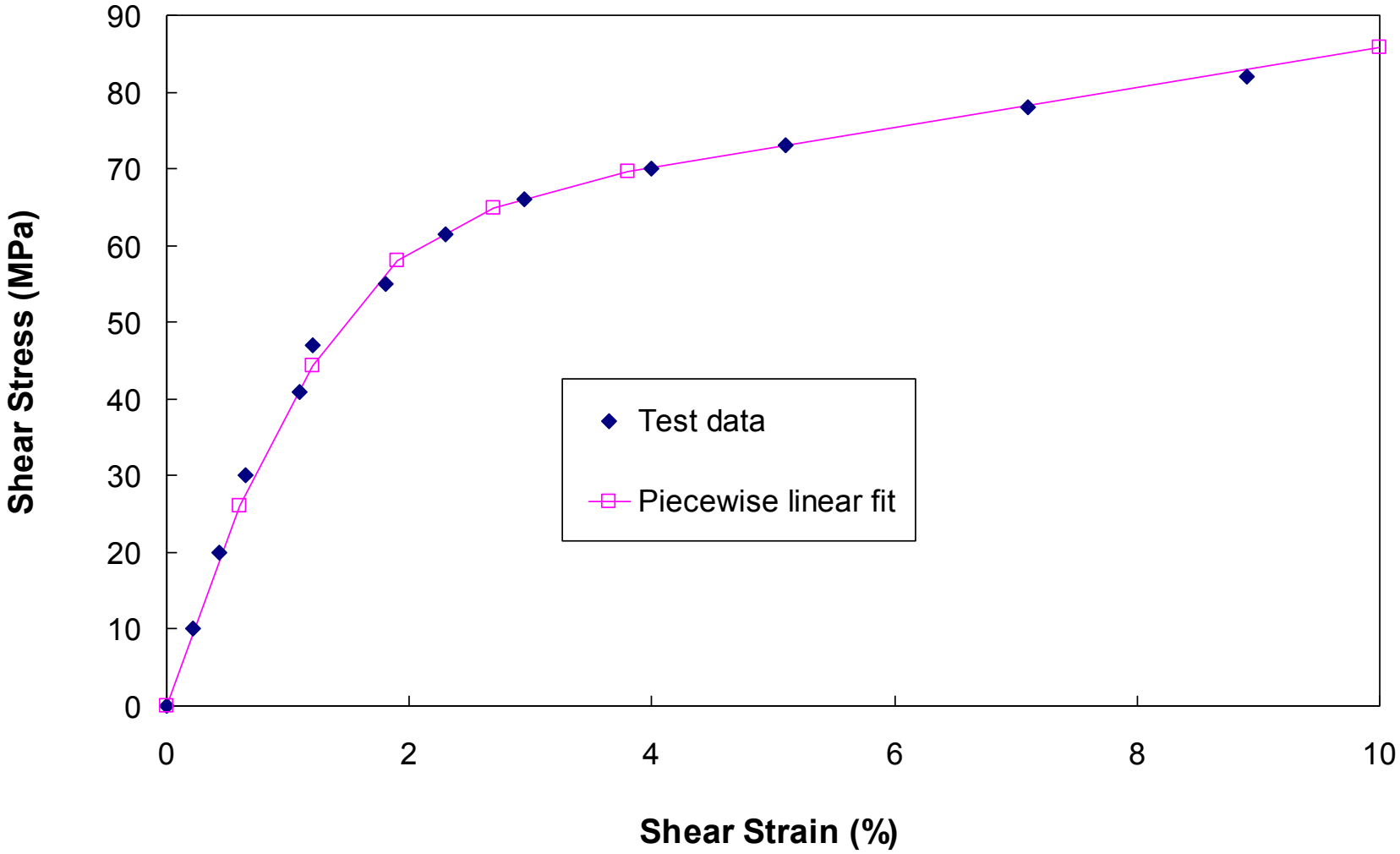

Figure 7 Test data from reference 21 and piecewise linear fit used in the analysis

a

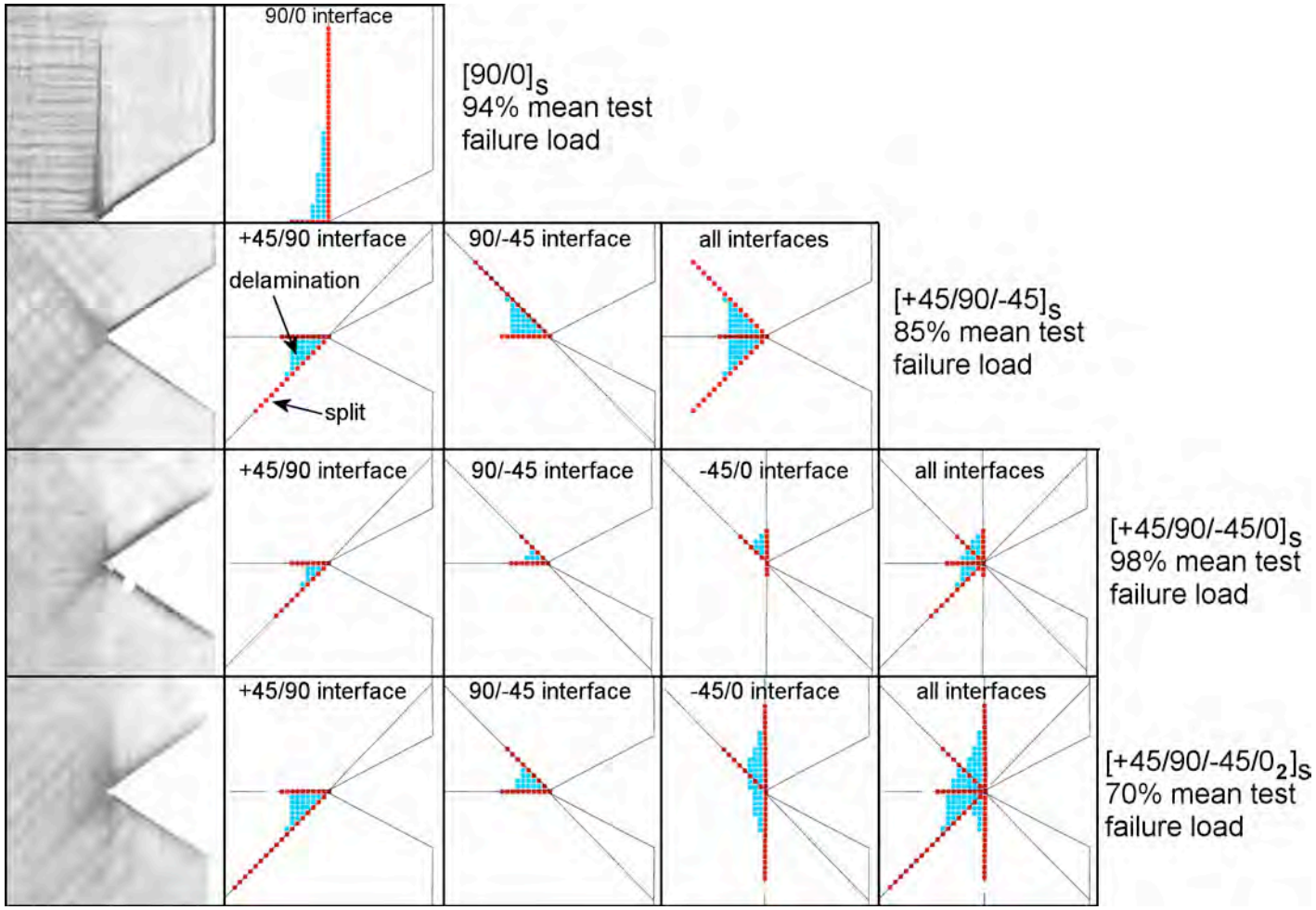

Figure 8 Results for delamination and split location for different lay-ups tested and modelled

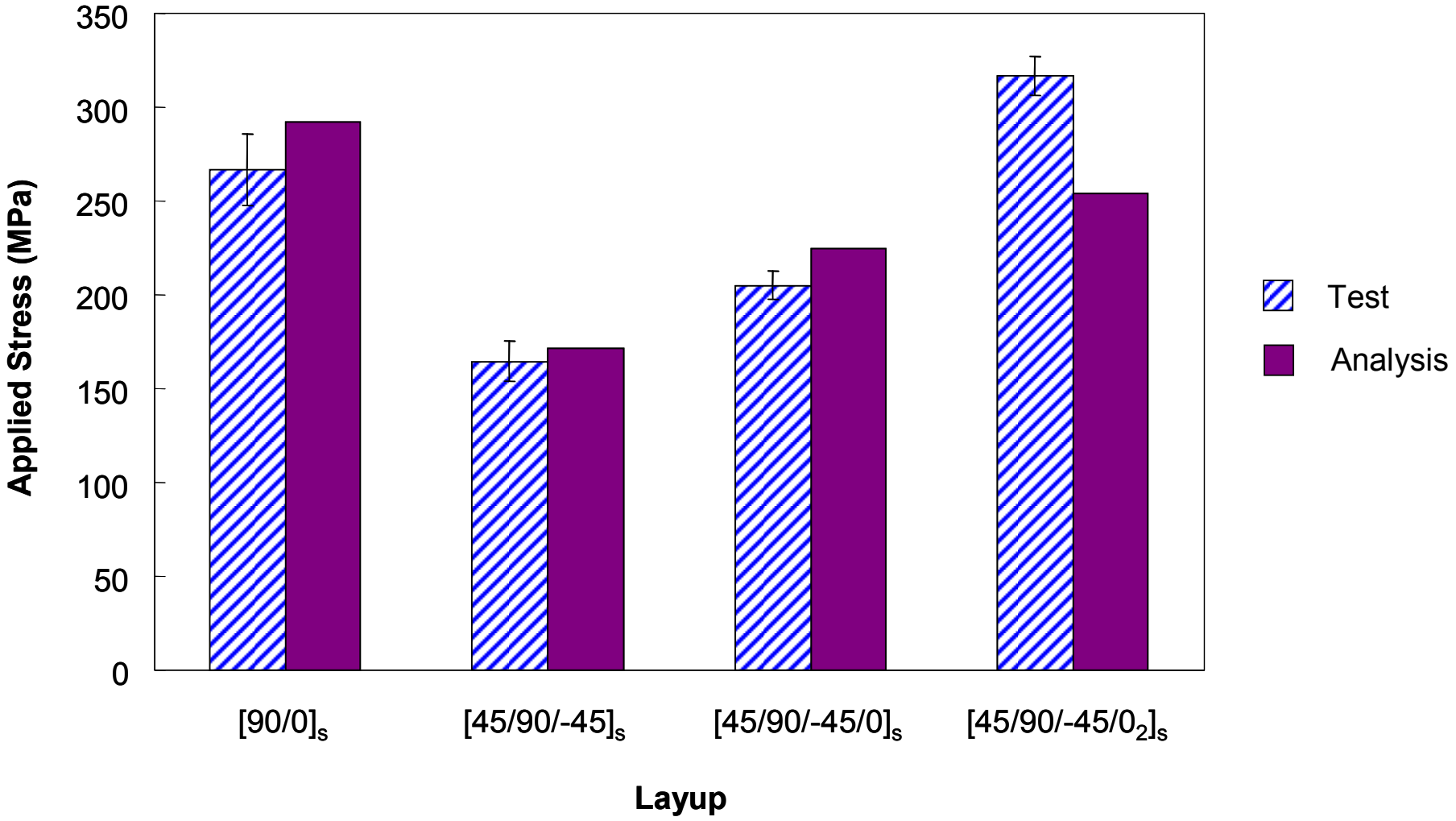

Figure 9 Ultimate failure stress for 20mm wide specimens test to analysis correlation

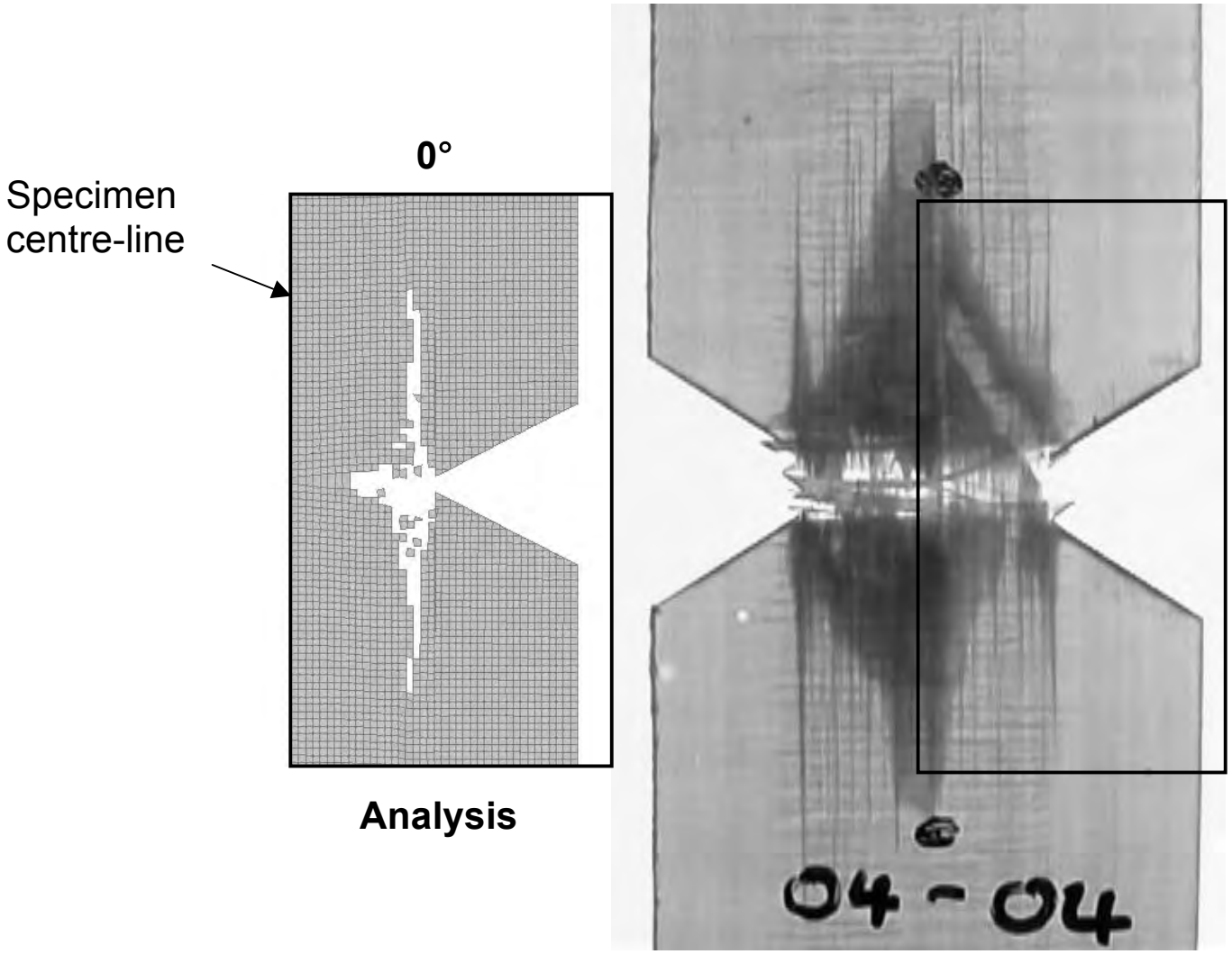

Figure 10 Failure of the 20mm wide cross-ply specimen

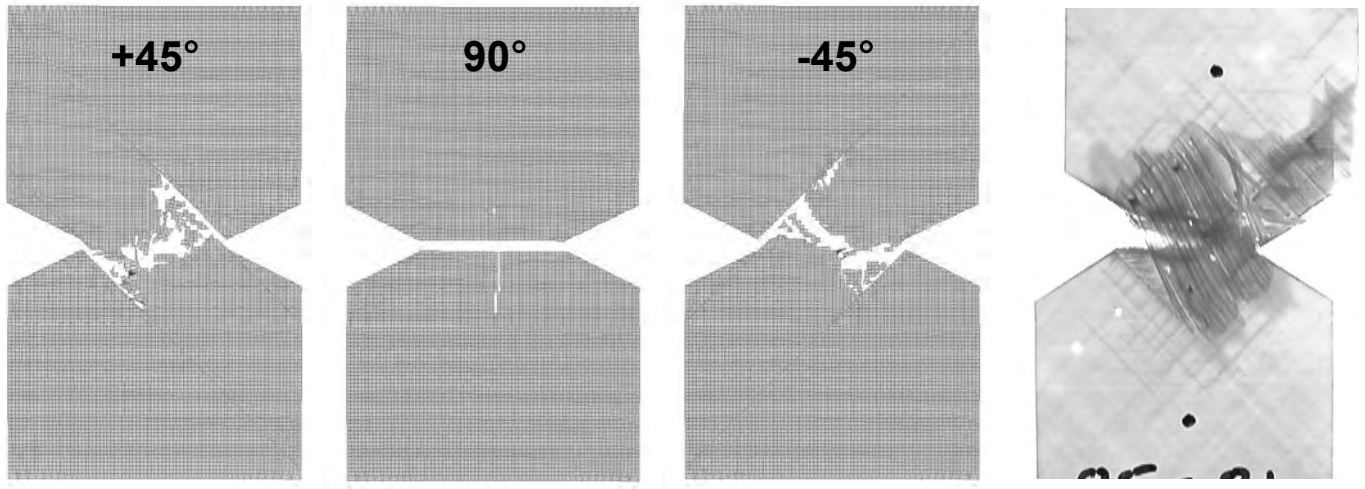

Figure 11 Failure of the 20mm wide $[+45/90/-45]_s$ specimen showing fibre failure

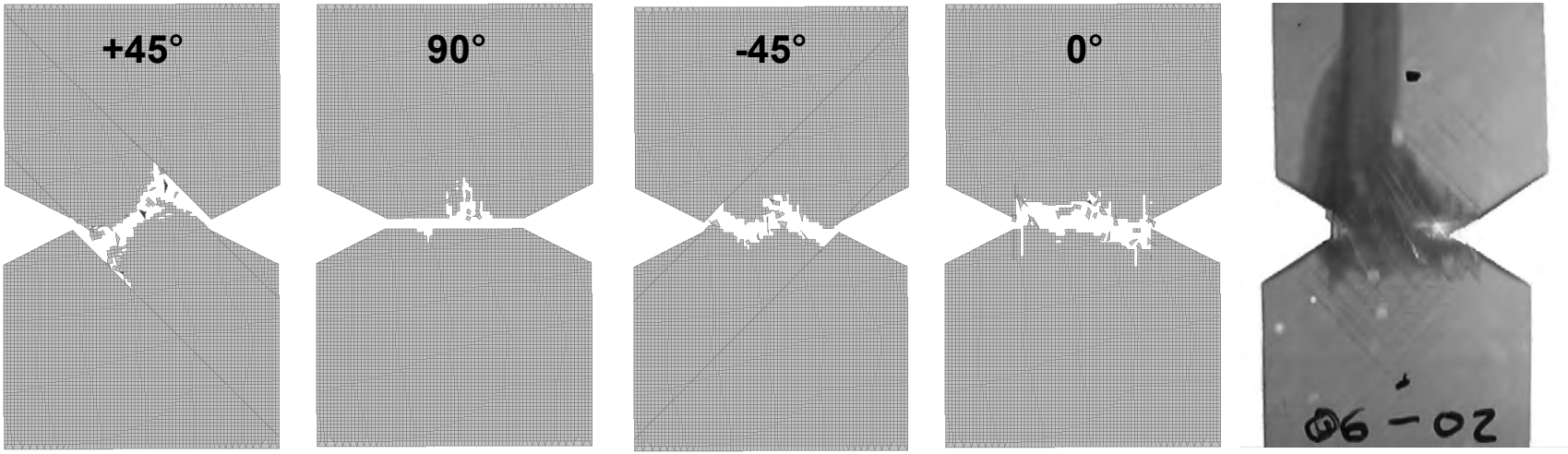

Figure 12 20mm wide $[+45/90/-45/0]_s$ layup analysis and test failure mode comparison

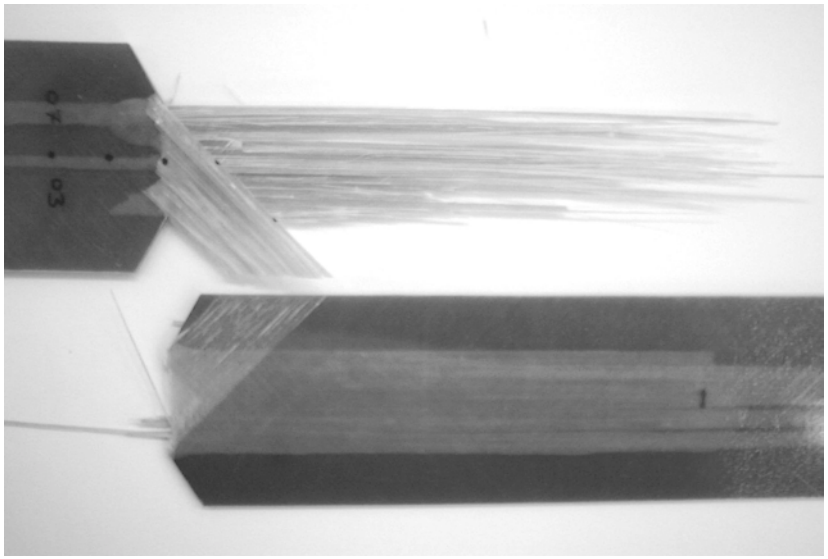

Figure 13 Photograph of 40mm wide $[+45/90/-45/0_2]_s$ specimen showing distributed failure[4]

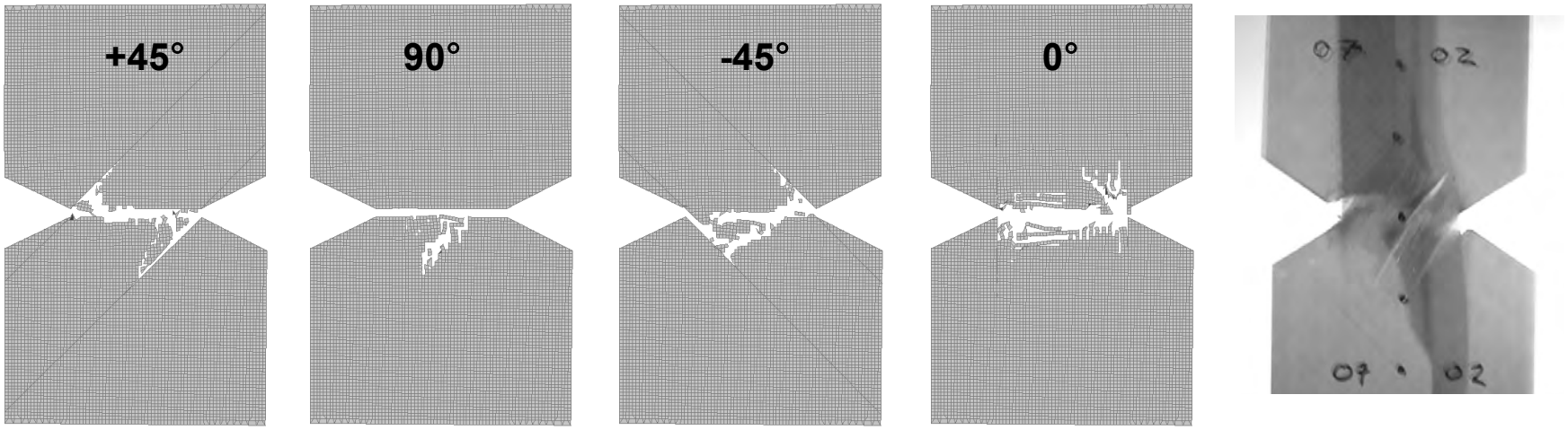

Figure 14 Failure pattern for the $[+45/90/-45/0_2]_s$ layup 20mm wide specimen

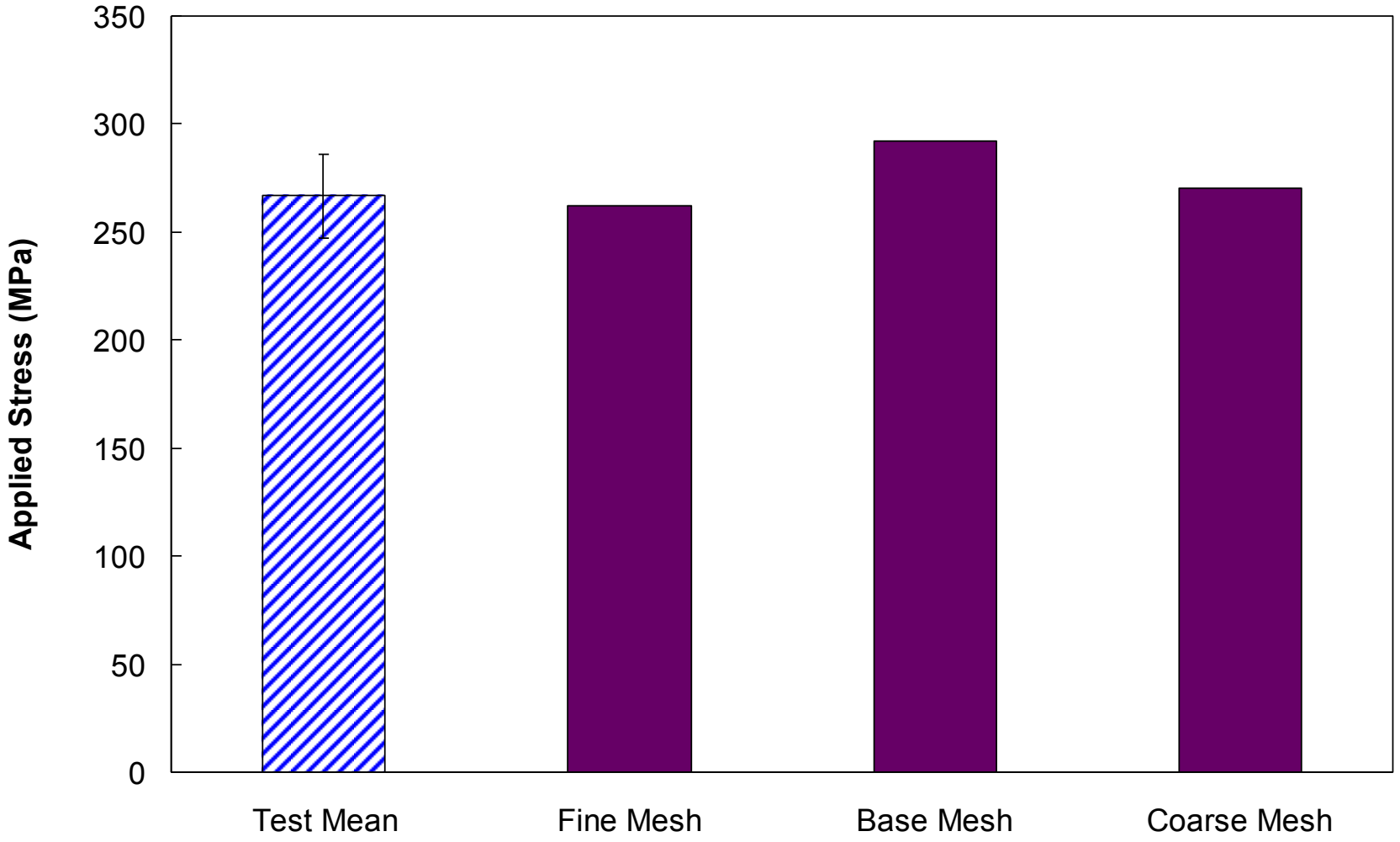

Figure 15 Failure stress for $[90/0]_s$ layup for different mesh sizes

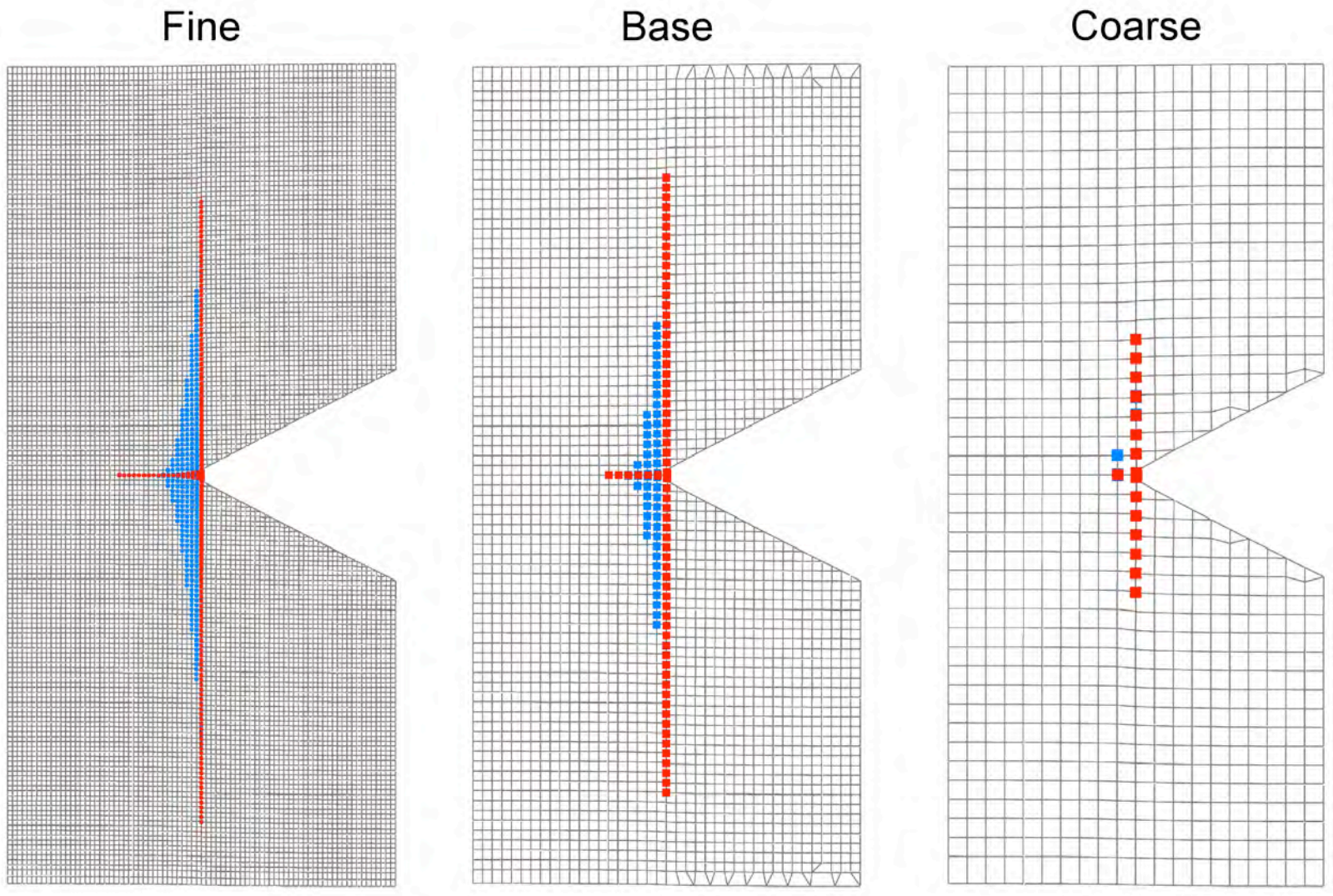

Figure 16 Effect of varying the mesh size